

Dilation Aware Multi-Image Enrollment for Iris Biometrics

Estefan Ortiz¹ and Kevin W. Bowyer¹

Abstract

Current iris biometric systems enroll a person based on the best eye image taken at the time of acquisition. However, recent research has shown that simply taking the best eye image and ignoring pupil dilation leads to degradations in system performance. In particular, the probability of a false non-match increases when there is a considerable variation in pupil size between the enrolled eye image and the probe eye image. Therefore, methods of enrollment that take into account pupil dilation are needed to ensure reliability of an iris biometric system. Our research examines a strategy to improve system performance by implementing a dilation-aware enrollment phase that chooses eye images based on their respective empirical dilation ratio distribution. We compare our strategy of enrollment to that of the randomly chosen eye images, which is the current enrollment procedure for most iris biometric systems. Our results show that there is a noticeable improvement over the random scenario when pupil dilation is accounted for during the enrollment phase.

1. Introduction

Recent research has shown that the performance of an iris biometric system tends to degrade when large variations in pupil dilation exist between the enrolled iris image and the iris image to be recognized or verified [1-3]. In particular, Hollingsworth et al. [1] demonstrated that when the pupil dilation of the enrolled iris image and probe iris image differ, the number of false non-matches tend to increase. The degradation in current system performance found in [1] was also verified by the National Institute of Standards and Technology (NIST) [3] in a larger study of iris biometric systems. In particular, the NIST study examined the effects of pupil dilation across multiple datasets using various commercial iris biometric software. To account for the degradations in system performance due to pupil dilation each study recommended that knowledge

of pupil dilation be incorporated into an iris biometrics system either at the enrollment phase or decision phase.

Hollingsworth suggested including meta-data that specifies the degree of pupil dilation for each enrolled iris image. The pupil dilation meta-data could then be used to assign a reliability measure to the match score of two iris codes. At the final decision phase, the reliability measure would then be used to determine the best match for a given probe against the gallery of iris codes. While Hollingsworth suggested including meta-data based on pupil dilation that could be used in determining a final match, the NIST report recommended an approach aimed at the enrollment phase of an iris biometric system. In particular, the NIST study proposed enrolling a person with multiple iris images with varying degrees of pupil dilation to help offset the detrimental effects pupil dilation has on the performance of an iris biometric system.

Following the recommendations of the NIST report, we examine a method of enrolling multiple iris images with varying degrees of pupil dilation. The approach developed determines the iris images for enrollment based on the empirical pupil dilation distribution for the respective eye of a given subject. Presented in this paper is an investigation of using pupil dilation information via the respective empirical distribution as part of the enrollment phase of an iris biometric system.

1.1. Background

The main purpose of an iris is to vary the diameter of the pupil in order to control the amount of light that can enter the eye. The primary mechanism the iris uses to change the dilation size of the pupil are the sphincter muscles and the dilator muscles. The sphincter muscles constrict the pupil (decrease the size of pupil dilation) while the dilator muscles expand the size of the pupil. In both operations (constriction and dilation) the texture and shape of the iris surface undergoes changes due to the behavior of the sphincter and dilator muscles [3,4]. The change in texture surface of an iris is particularly important to biometric systems that are based on identifying and using patterns found within the iris.

The most widely used approach to iris biometrics was developed by Daugman [5-7]. In general, Daugman's method consists of five main stages: 1.) capturing an image of the eye in the near infrared spectrum; 2.) segmenting the

¹ Department of Computer Science and Engineering, University of Notre Dame, 384 Fitzpatrick Hall, Notre Dame, IN 46556, USA
{eortiz, kwb}@nd.edu

eye image to find the iris texture area; 3.) normalizing and unwrapping the iris texture area to a rectangular grid of a fixed pixel resolution; 4.) filtering the unwrapped image to find the most representative textures; and 5.) encoding the texture information to a binary code also called an iris code. For an in depth discussion on the development of iris biometrics and respective commercial and research iris recognition technologies refer to [5-8]. The final phase of an iris biometric system is the construction of a database for iris codes of different individuals.

The process of populating a database consisting of iris codes from various individuals is referred to as gallery construction or more specifically iris image enrollment. In most iris biometric systems individuals have one or both of their eyes processed and their iris code included in a database. Once a gallery has been constructed it can be used for identification or verification purposes at a later time. In either identification or verification the similarity measure used to compare two iris codes is the fractional Hamming distance as defined in [6]. In general, the fractional Hamming distance counts the number of disagreeing bits between two iris codes and normalizes the count by the number of bits used for comparison. The described method of iris biometrics has shown to perform well for a large class of eye images. However, system performance begins to degrade when the difference in pupil dilation size between eye images used for enrollment and those used to test the system becomes large.

In the Daugman method, fluctuations of the iris texture due to pupil variation are accounted for by the normalization phase. Changes of iris texture surface are modeled by assuming that variations in texture occur in a linear fashion. As described in [6], invariance of the iris texture mapping can be achieved by the translation of the captured data to a double dimensionless pseudo-polar coordinate system. The model used to account for iris texture change is generally referred to as a “homogenous rubber-sheet model”. The rubber sheet model has been shown to be a good representation of iris texture for moderate pupil dilation changes. However, research has shown that when differences in the pupil dilation between the enrolled iris image and the probe image grow, errors in performance begin to increase. As a result, it is speculated that the rubber sheet model may not adequately account for nonlinear texture changes due to large variations in pupil dilation.

As a visual example Figure 1(a) and Figure 1(b) show the left eye of a given subject at two different dilation degrees. From Equation (1) the dilation ratio found for Figure 1 (a) is 0.3832 and Figure 1 (b) the dilation ratio is 0.6423. The two eye images seen in Figure 1 display the considerable change in iris texture due to pupil dilation.



Figure 1: Eye images of Subject nd1S0583. (a) Pupil dilation ratio of: 0.3832. (b) Pupil dilation ratio of: 0.6423

The effect that pupil dilation has on the performance of an iris biometric system was examined in [1]. Their research found that as the variation in pupil dilation between the enrolled eye image and the probe image increased, so too did the number of false non-matches. The most noticeable performance degradation came at the largest variation in pupil dilation size. Their findings were also confirmed independently by a NIST study [3] into iris biometric systems. In both instances it was recommended that knowledge of pupil dilation be incorporated into an iris biometric system to prevent such degradations. This paper examines a way in which eye images can be chosen for enrollment based on pupil dilation. In particular, we study the performance of choosing eye images based on the empirical distribution function of the dilation ratios.

2. Dilation Aware Enrollment

The material found in the following sections detail the background and methodology used to incorporate pupil dilation information into a biometric system. Section 2.1 covers the measure and empirical distribution function for pupil dilation. Section 2.2 and Section 2.3 describe the iris image enrollment methodologies used for analysis.

2.1. Pupil Dilation

The dilation ratio described in [1] is used as the measure for pupil dilation. The measure is defined in terms of the pupil and iris radii found from the segmentation phase. Specifically, pupil dilation is measured as the ratio of pupil radius to iris radius given as,

$$\Delta = \frac{\text{pupil radius}}{\text{iris radius}} \quad (1.)$$

The calculated pupil dilation ratio Δ of a segmented eye image will also be referred as the dilation ratio throughout this paper. While the pupil dilation ratio can in principle vary between zero and one, the range of values experienced in practice is from about 0.2, representing a highly constricted pupil, to about 0.7, representing a highly dilated pupil. To use pupil dilation as a part of the enrollment phase

of an iris biometric system, we examine the empirical distribution function found from dilation ratio samples. In analysis it is assumed that there are an adequate number of eye image samples such that a probability distribution can be estimated and used for enrollment purposes.

For a particular subject who has multiple iris images available for enrollment, the probability distribution of dilation ratios can be estimated from the empirical distribution function. The empirical distribution function is calculated from the dilation ratios found over each of the available iris images for the respective eye (Left or Right). Following [9], assume the observations X_1, \dots, X_n are independent and identically distributed with a common cumulative distribution function $F(x)$. The order statistic of the observations are denoted with the parenthetical subscript such that $X_{(1)} < X_{(2)} \dots < X_{(n)}$. Where $X_{(1)}$ and $X_{(n)}$ are the minimum and maximum respectively. The empirical distribution function $F_n(x)$ corresponding to the n observations is defined by the order statistics given as,

$$F_n(x) = \begin{cases} 0, & x \leq X_{(1)} \\ i/n, & X_{(i)} < x < X_{(i+1)}, 1 \leq i \leq n-1 \\ 1, & x > X_{(n)} \end{cases} \quad (2.)$$

In terms of enrolling eye images through the statistical properties of their dilation ratio, the empirical distribution can be directly used.

We examine two types of enrollment methodologies to determine if there is an improvement due to the inclusion of iris images that have varying pupil dilation ratios. The two methods are referred to as random enrollment and quantile enrollment. The quantile process of enrolling iris images directly uses statistical information from the empirical distribution function. It is a structured way in which to include information about pupil dilation into the enrollment phase. Random enrollment is used as a comparison to model the enrollment process of most iris biometric systems. Specifically, random enrollment does not take into account any knowledge of pupil dilation when determining which iris image to enroll. Both enrollment strategies are discussed in the following sections.

2.2. Random Enrollment

The gallery constructed based on random enrollment mimics the enrollment process for most iris biometric systems. Meaning, for each subject an iris image is chosen at random without regard to pupil dilation. If more than one iris image is allowed per subject in the gallery, the random

enrollment process samples iris images without replacement. Figure 2(a) displays the random enrollment process for the case in which three iris images are allowed in the gallery for each subject.

2.3. Quantile Enrollment

In contrast to random enrollment, the quantile enrollment strategy uses pupil dilation information to decide which eye images should be included in the gallery for a given individual. The general idea behind the quantile enrollment is to choose eye images for a given subject based on the empirical distribution of their pupil dilation ratios. In particular, quantile enrollment is accomplished by choosing the iris images that are associated to the points taken at equal intervals from the empirical distribution of the dilation ratios. It divides the ordered data into q equal sized subsets. The points denoting the boundaries of consecutive subsets are commonly known as the quantiles. In terms of the empirical distribution, the k^{th} quantile for the random variable X is value x such that,

$$F_n(x) = k/q, \quad 0 < k < q. \quad (3.)$$

Following [9], the equally spaced points of the empirical distribution are given by the realization sequence of the order statistics as defined in Section 2.1. Where x_1, \dots, x_n is considered to be a realization of the random sequence X_1, \dots, X_n , and $x_{(1)} < x_{(2)} \dots < x_{(n)}$ is a realization of the order statistics. In general, let $p \in (0,1)$ with the sample quantile associated to p specified by the rank statistic whose index is $p(n+1)$. Since $p(n+1)$ may not have an integer value we let $j = \lfloor p(n+1) \rfloor$ be the integer part of the desired rank. Where $\lfloor \cdot \rfloor$ is the floor function. Correspondingly, $t = p(n+1) - j$ is defined as the fractional part of the desired rank. Therefore, the sample quantile x_p of order p is given as the following interpolated value.

$$x_p = (1-t)x_{(j)} + tx_{(j+1)}. \quad (4.)$$

Therefore, quantile enrollment chooses m iris images for the gallery that are near the m quantile points found by segmenting the ordered observations into $m+1$ equal subsets. To simulate the behavior of this process the quantile points are used as a reference in which to randomly

sample iris images that have pupil dilations near the defined quantile points. Section 4 discusses this in detail.

To illustrate the quantile method for enrollment, assume three iris images are to be used for enrollment for a given subject. The empirical distribution of the dilation ratios calculated from the eye image samples is divided into four equal subsets with three quantiles division points corresponding to the 0.25, 0.50 and 0.75 quantiles. The three eye images with pupil dilation ratio values that are the closest in terms of absolute difference to the quantile points are chosen as the enrolled eye images for that particular subject. Conceptually, Figure 2(b) displays the quantile enrollment process for the case when three iris images are allowed per subject.

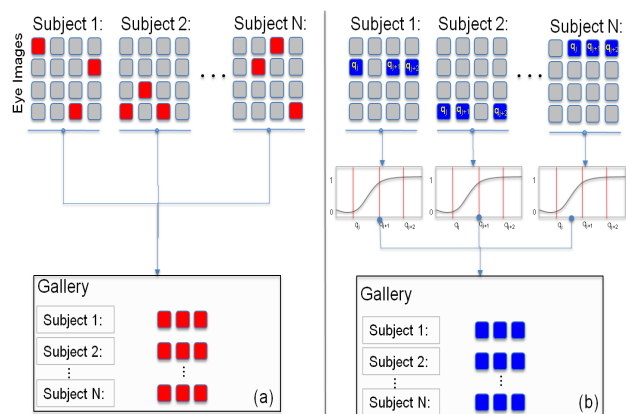


Figure 2: Random Enrollment (a). Quantile Enrollment (b)

3. Data and Software

To evaluate each of the enrollment strategies described in Section 2.2 and Section 2.3, iris image data collected at the University of Notre Dame between 2008 and 2010 using the LG IrisAccess 4000 camera was used. The dataset consists of 294 unique subjects with 10,823 left eye iris images and 10,885 right eye images. Each subject used in the study had at least twenty eye images per eye. The data contained subjects which ranged from 18 years of age to 63 years of age, with a median age of 22 years old.

The software used for segmentation and encoding of raw eye images was based on the implementation of Masek [10] and modified and updated by Liu [11]. The applied software implements a version of the general approach to iris biometrics due to Daugman [5-7] and Wildes [12]. The software implements a Canny edge detector to determine the limbus and pupillary boundaries. The iris texture area is considered to be the segment bounded by the limbus and pupillary demarcations. The iris texture area is unwrapped and normalized to a rectangular grid of a fixed size. The normalized iris image is filtered using a bank of log-Gabor filters. The log-Gabor filters are used to represent the texture information contained within the normalized iris

image. The texture information found through the filtering stage is then mapped to a binary code based on the phase information of the complex filter outputs. The final iris code size for a processed iris image is 10x240 bits. For each iris image the pupil dilation ratio information is calculated using Equation 1.

3.1. Pupil Dilation Ratio Statistics

The aggregate distribution of the pupil dilation ratios per eye can be seen in Figure 3. The pupil dilation histograms for each eye location found in Figure 3 show that there is a wide distribution in dilation ratios across all of the subjects within the dataset.

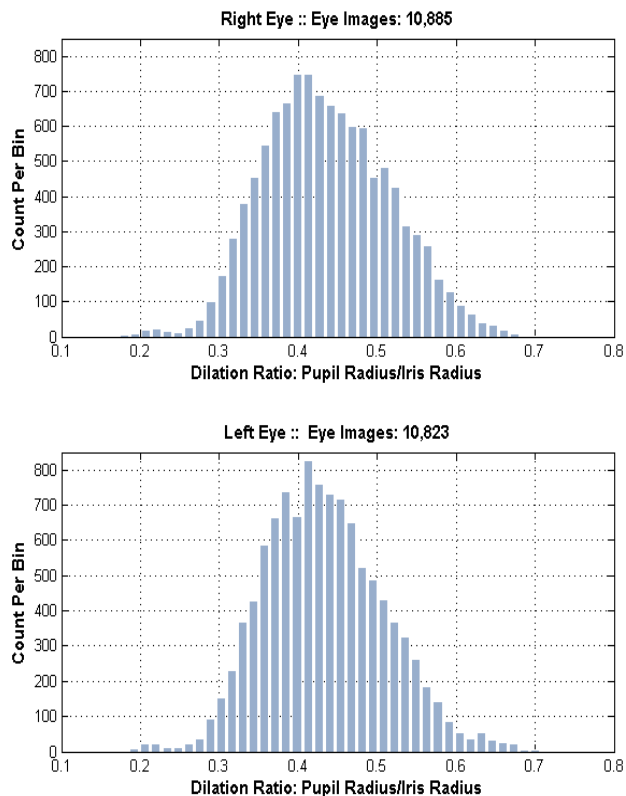


Figure 3: Distribution of dilation ratios for each eye location of the sampled subjects for the LG4000

4. Experimental Method

To evaluate the random and quantile methods of iris image enrollment we examine the performance of enrolling multiple eye images for each subject. In construction of each gallery type, it is assumed that every subject will be represented by m iris images determined by the respective enrollment methods. A given experiment examines the effect of a specified number of iris images to be enrolled for each subject. For instance, if there are 294 subjects to be enrolled in the gallery each will have m enrolled iris

images for a total of 294 m enrolled iris images in the gallery.

To estimate the behavior of incorporating pupil dilation information within the enrollment phase, the quantile enrollment method finds for each subject the m quantiles for their respective iris images. For a particular dilation ratio quantile, a single iris image is randomly selected from the set of iris images that have dilation ratio values within a 1% tolerance range of the quantile value. Thus, the quantile gallery will have m iris images that are representative of the calculated quantile values. In contrast, the random gallery is constructed by sampling m iris images for each subject without regard to pupil dilation.

For a given simulation iteration the iris images used in building both the random and quantile galleries are removed from the testing set. Additionally, the corresponding iris images acquired on the same day as those used for enrollment are also removed from the testing set. The samples that remain for each subject are used as a common probe set for testing. The fractional Hamming distance defined in [6] is used to calculate the distance between gallery and probe set iris codes. The described simulation process is iterated 300 times for a varying enrollment size of 1 to 4 iris images per subject per eye location (Left and Right). The match and non-match distances are calculated using the fractional Hamming distance. The match and non-match distances found and are used to produce a receiver operating characteristic (ROC) curve. The ROC curve for a given iteration is estimated by varying the decision threshold of fractional Hamming distance values from 0 to 1 in linear step sizes of 1/300 and calculating the false accept rate (FAR) and true accept rate (TAR) at each threshold value. We aggregate the FAR and TAR values for each threshold value to calculate the average ROC curve behavior. Under normality assumptions for each threshold value, we estimate the mean FAR and TAR and respective 95% confidence intervals.

4.1. Results

Figures 4-7 display the average ROC curves of the quantile and random enrollment methods for the enrollment sizes of 1 to 4 iris images per subject. In each ROC plot we display the estimated mean FAR and TAR for each of the threshold values. In each graph the confidence interval for the mean TAR is plotted as lines about the solid curves. In terms of performance, an accurate process should have an ROC curve that quickly rises and is oriented toward the left-hand border. We found that in each experiment the quantile enrollment strategy outperformed the scenario in which random eye images are used for enrollment. However, we note the case where two images are allowed per subject Figure 5. In this case there was only a slight gain performance. This may be due to the observation that the quantiles chosen as enrollment points are wide and

excluded eye images corresponding to the median dilation or the 0.5 order quantile value. In each of the other experiments the median is used or there were enough divisions such that the omission of the median did not affect performance. From Figures 4-7 we can also see that the performance difference between the two enrollment strategies becomes smaller. This is primarily a result of having a greater chance of a match due to an increased number of iris images per subject in the gallery.

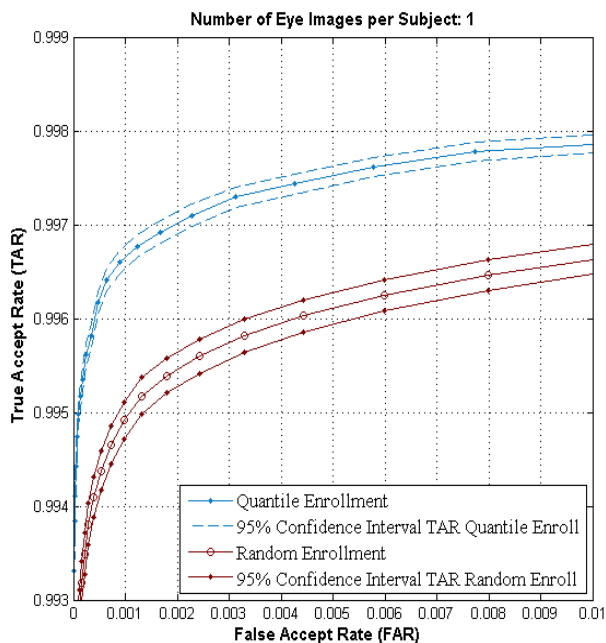


Figure 4: ROC of quantile enrollment and random enrollment number for 1 iris image selected per subject.

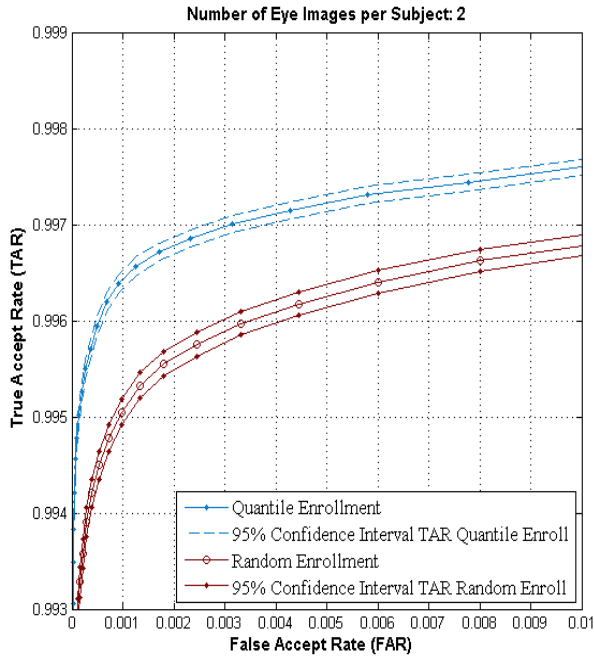


Figure 5: ROC of quantile enrollment and random enrollment number for 2 iris images selected per subject.

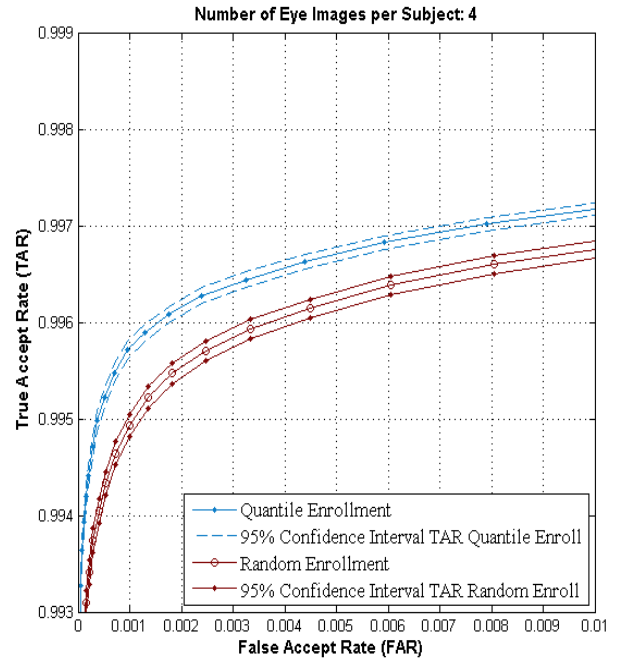


Figure 7: ROC of quantile enrollment and random enrollment number for 4 iris images selected per subject.

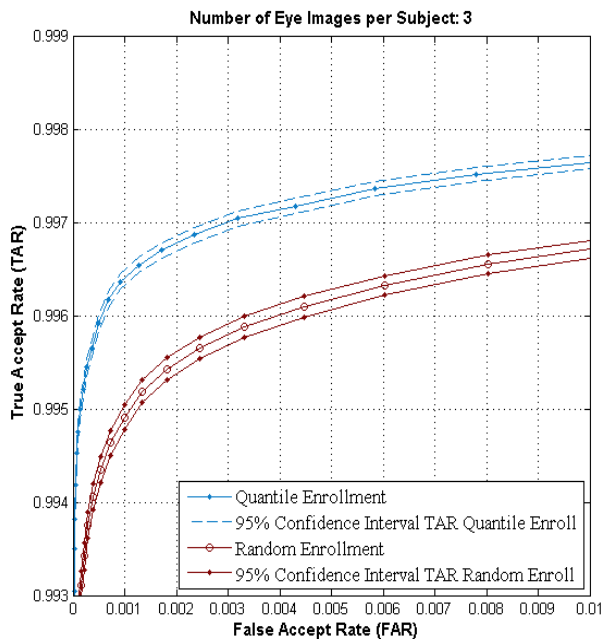


Figure 6: ROC of quantile enrollment and random enrollment number for 3 iris images selected per subject.

5. Conclusions

We found that the incorporation of pupil dilation information into the enrollment phase resulted in a noticeable improvement over the random selection strategy. The largest observed performance gain was in the case of choosing a single iris image for the gallery. This leads us to conclude that if we are allowed only one iris image per subject for the gallery the iris image with the median pupil dilation ratio should be selected for enrollment.

6. Future Work

The research presented was focused primarily on the enrollment phase of an iris biometric system. The next natural step to take in advancing the idea of incorporating pupil dilation in a complete iris biometric system is to develop a decision strategy that also uses information regarding pupil dilation. It would be beneficial to examine and abstract at the decisions phase those factors that degrade performance in an iris recognition system. And much like the process examined in this study use that information to possibly improve overall performance.

7. Acknowledgement

This research was funded by the Office of the Director of National Intelligence (ODNI), Intelligence Advanced Research Projects Activity (IARPA), through the Army Research Laboratory (ARL). The views and conclusions contained in this document are those of the authors and should not be interpreted as representing official policies, either expressed or implied, of IARPA, the ODNI, the Army Research Laboratory, or the U.S. Government. The U.S. Government is authorized to reproduce and distribute reprints for Government purposes notwithstanding any copyright notation herein. The opinions, findings, and conclusions or recommendations expressed in this publication are those of the authors and do not necessarily reflect the views of our sponsors.

References

- [1] K. Hollingsworth, K. Bowyer, and P. Flynn. Pupil dilation degrades iris biometric performance. *Computer Vision and Image Understanding*, 113(1):150–157, 2009.
- [2] Karen Hollingsworth, Kevin Bowyer, Patrick Flynn, The importance of small pupils: a study of how pupil dilation affects iris biometrics, in: *Biometrics: Theory, Applications, and Systems*, September 2008.
- [3] P. Grother, E. Tabassi, G.W. Quinn, and W. Salamin. IREX I: Performance of Iris Recognition Algorithms on Standard Images. NIST Technical Report, National Institute of Standards and Technology, Gaithersburg, Maryland. October 30, 2009.
- [4] S. S. Phang. *Investigating and developing a model for iris changes under varied lighting conditions*. PhD thesis, Queensland University of Technology, 2007.
- [5] J. Daugman. New methods in iris recognition. *IEEE Transactions on Systems, Man, and Cybernetics, Part B*, 37(5):1167–1175, October 2007.
- [6] John Daugman. How iris recognition works. *IEEE Transactions on Circuits and Systems for Video Technology*, 14(1):21–30, January 2004.
- [7] John Daugman, High confidence visual recognition of persons by a test of statistical independence, *IEEE Transactions on Pattern Analysis and Machine Intelligence* 15 (11) (1993) 1148–1161.
- [8] K.W. Bowyer, K.P. Hollingsworth, P.J. Flynn, Image understanding for iris biometrics: a survey, *Computer Vision and Image Understanding* 110 (2) (2008) 281–307.
- [9] M. Ahsanullah, V. B. Nevzorov “Order statistics: examples and exercises” Nova Science Pub Inc (June 2004)
- [10] Libor Masek, Peter Kovesi, MATLAB source code for a biometric identification system based on iris patterns, The University of Western Australia, 2003. Available from: <<http://www.csse.uwa.edu.au/~pk/studentprojects/libor/>>.
- [11] Xiaomei Liu, Kevin W. Bowyer, Patrick J. Flynn, Experiments with an improved iris segmentation algorithm, in: *Fourth IEEE Workshop on Automatic Identification Technologies*, October 2005, pp. 118–123.
- [12] Richard P. Wildes, Iris recognition: an emerging biometric technology, *Proceedings of the IEEE* 85 (9) (1997) 1348–1363.